On Implementation of the Finite Difference Lattice Boltzmann Method with Internal Degree of Freedom to Edgetone

Hokeun Kang*
School of Mechanical and Aerospace Engineering · Institute of Marine Industry, Gyeongsang National University, 445 Inpyeong-dong, Tongyeong, Gyeongnam 650-160, Korea
Eunra Kim
Department of Civil Engineering · Research Center of Industrial Technology, Chonbuk National University, 664-14 1ga Duckjin-Dong Duckjin-Gu Jeonju Jeonbuk 561-756, Korea

The lattice Boltzman method (LBM) and the finite difference-based lattice Boltzmann method (FDLBM) are quite recent approaches for simulating fluid flow, which have been proven as valid and efficient tools in a variety of complex flow problems. They are considered attractive alternatives to conventional finite-difference schemes because they recover the Navier-Stokes equations and are computationally more stable, and easily parallelizable. However, most models of the LBM or FDLBM are for incompressible fluids because of the simplicity of the structure of the model. Although some models for compressible thermal fluids have been introduced, these models are for monatomic gases, and suffer from the instability in calculations. A lattice BGK model based on a finite difference scheme with an internal degree of freedom is employed and it is shown that a diatomic gas such as air is successfully simulated. In this research we present a 2-dimensional edge tone to predict the frequency characteristics of discrete oscillations of a jet-edge feedback cycle by the FDLBM in which any specific heat ratio γ can be chosen freely. The jet is chosen long enough in order to guarantee the parabolic velocity profile of a jet at the outlet, and the edge is of an angle of $\alpha=23^0$. At a stand-off distance w, the edge is inserted along the centerline of the jet, and a sinuous instability wave with real frequency is assumed to be created in the vicinity of the nozzle exit and to propagate towards the downstream. We have succeeded in capturing very small pressure fluctuations resulting from periodic oscillation of the jet around the edge.

Key Words : Finite Difference Lattice Boltzmann Method, Edgetone, Feedback

1. Introduction

Developed from the lattice gas automata (LGA or lattice gas cellular automaton, LGCA) (Wolfram, 1986) model, the lattice Boltmann method (LBM) (Alexander et al., 1993 ; Chen & Doolen, 1998 ; Tsutahara et al., 1999) is a quite recent approach for simulating fluid flow, which has been proven to be a valid and efficient tool in a variety of complex flow problems. In traditional numerical methods, the macroscopic variables, velocity and density, are obtained by solving the Navier-Stokes equations. The lattice Boltzmann method, however, solves the microscopic kinetic

* Corresponding Author,
E-mail : kang88@gaechuk.gsnu.ac.kr
TEL : +82-55-640-3064; **FAX** : +82-55-640-3120
School of Mechanical and Aerospace Engineering · Institute of Marine Industry, Gyeongsang National University, 445 Inpyeong-dong, Tongyeong, Gyeongnam 650-160, Korea. (Manuscript **Received** January 12, 2005; **Revised** September 9, 2005)

equation for particle distribution function from which the particles move at unit speed on a regular grid subject to particle movement and simplified collision rules, which conserve the total fluid mass, momentum and energy. The presently popular method uses regularly spaced lattices and is difficult to handle curved boundaries with desirable flexibility. To circumvent such difficulties, the finite difference-based lattice Boltzmann method (FDLBM) (Cao et al., 1997) and the finite volume-based lattice Boltzmann method (FVLBM) (Peng et al., 1999) in curvilinear coordinates are applied using body-fitted coordinates with non-uniform grids. Especially, FDLBM makes it possible and easy to simulate complicated object shapes, and the applications to various flow fields are attained. This method has high flexibility for coordinate system selection and is often the choice among various schemes.

However, most models in LBM or conventional FDLBM are incompressible fluids because of the simplicity of the structure of the model. Although some models for compressible thermal fluids have been introduced, these models are for monatomic gases, and suffer from the instability in calculation.

In the present work, in order to apply the finite difference lattice Boltzmann model to simulate such as diatomic gases, air, etc., a lattice BGK model with an internal degree of freedom, which was introduced to the LBM by Takada & Tsutahara (1999), is employed to predict a speed of sound. Then, we simulate the modified model to the onset issue for an edgetone generated by a two-dimensional jet impinging on a wedge to predict frequency characteristics of the discrete oscillation of a jet-edge feedback cycle. As a result, the model with an internal degree of freedom can be easily used to simulate complex fluid flows and associated transport phenomena such as aeroacoustics.

2. Computational Methodology

2.1 Finite difference lattice Boltzmann model with internal degree of freedom

The Boltzmann equation governing the velocity distribution function f_i may be written, with single relaxation time ϕ, as:

$$\frac{\partial f_i}{\partial t}+\boldsymbol{c}_i\cdot\nabla f_i=-\frac{1}{\phi}(f_i-f_i^{eq}) \tag{1}$$

Here, the real number f_i is the normalized number of particles at each lattice node and time t, moving direction i. Furthermore, to apply for high Reynolds number and speed up the calculation time, the modified equation (Kang et al., 2002) in which the third term is added to the discretized BGK equation (Eq.(1)) is transformed as:

$$\frac{\partial f_i}{\partial t}+\boldsymbol{c}_i\cdot\nabla f_i-Ac_i\cdot\frac{f_i-f_i^{eq}}{\phi}=-\frac{1}{\phi}(f_i-f_i^{eq}) \tag{2}$$

in which $A(>0)$ is a constant, and other variables are the same as in Eq.(1).

When the energy equation is derived from Eq. (2), the ratio of specific heats γ in BGK model is expressed by the degree of freedom of the particle motion, which, in this conventional model, corresponds to the dimensional number D, as:

$$\gamma=(D+2)/D \tag{3}$$

It is well known that the degree of freedom coincides with the dimension, and in a two-dimensional case $\gamma=2$ and in a three-dimensional case $\gamma=1.67$ for monatomic gases, respectively, which are unrealistic. Therefore, in order to simulate realistic gases in two-dimension or three-dimension cases for diatomic gases, an additional internal degree of freedom should be considered.

To begin with, we apply the model having energy modes except the translation $G_i(\boldsymbol{x}, t)=f_i(\boldsymbol{x}, t)E_i(\boldsymbol{x}, t)$ to give the particle internal degree of freedom, which was proposed by Takada & Tsutahara (1999) in LBM. The distribution function $G_i(\boldsymbol{x}, t)$ is assumed to approach by collisions to its local equilibrium state $G_i^{eq}(\boldsymbol{x}, t)$ as the particle distribution functions do, and the evolution of $G_i(\boldsymbol{x}, t)$ is transformed as follows.

$$\frac{\partial G_i}{\partial t}+\boldsymbol{c}_i\cdot\nabla G_i-Ac_i\cdot\frac{G_i-G_i^{eq}}{\phi}=-\frac{1}{\phi}(G_i-G_i^{eq}) \tag{4}$$

Here, assumed that all the particles at the local

equilibrium stage have the same rotational energy as :

$$G_i^{eq}=Ef_i^{eq} \tag{5}$$

$$E=\frac{D}{2}\left(\frac{D+2}{D}-\gamma\right)e. \tag{6}$$

Here e is internal energy, and the specific heat ratio γ can be variable to $1.0<\gamma\leq 2.0$. Up to $O(u^3)$, we assume that the equilibrium distribution function f_i^{eq} in Eq. (5) is expressed as,

$$f_i^{eq}=F_i\rho[1-2B(\boldsymbol{c}_i\cdot\boldsymbol{u})+2B^2(\boldsymbol{c}_i\cdot\boldsymbol{u})^2+B(\boldsymbol{u}\cdot\boldsymbol{u}) -4/3B^3(\boldsymbol{c}_i\cdot\boldsymbol{u})^3-2B^2(\boldsymbol{c}_i\cdot\boldsymbol{u})(\boldsymbol{u}\cdot\boldsymbol{u})] \tag{7}$$

in which the subscript i refers to the kind of particles and B is represented by $B=-1/2(\gamma-1)e$. In a two-dimensional 21-speed particle model (D2Q21), the velocity of the particles is determined by :

$$c_i=k\sqrt{m}c\left[\cos\left(\frac{\pi(i-1)}{2}+\frac{\pi(i-1)}{4}\right), \sin\left(\frac{\pi(i-1)}{2}+\frac{\pi(i-1)}{4}\right)\right] \tag{8}$$
$$(i=1,\cdots,4,\ m=1,2,\ k=1,2,\cdots)$$

2.2 Macroscopic variables

The form of RHS term, given in Eq. (4), represents a relaxation of the distribution towards its equilibrium value and recovers the nonlinear form of the fluid, ensuring that the fully nonlinear Navier-Stokes equation is satisfied. The equilibrium distribution function f_i^{eq} depends on the fluid density ρ, velocity u, and internal energy e, at each site which can be calculated from the distribution functions as :

$$\rho=\sum_i f_i=\sum_i f_i^{eq} \tag{9}$$

$$\rho\boldsymbol{u}=\sum_i \boldsymbol{c}_i f_i=\sum_i \boldsymbol{c}_i f_i^{eq} \tag{10}$$

$$\frac{1}{2}\rho u^2+\rho e=\sum_i\left(\frac{1}{2}c_i^2 f_i+G_i\right) =\sum_i\left(\frac{1}{2}c_i^2 f_i^{eq}+G_i^{eq}\right) \tag{11}$$

The pressure, the second viscosity and the conductivity of internal energy are given, respectively, by :

$$p=(\gamma-1)\rho e \tag{12}$$

$$\mu=(\gamma-1)pe(\phi-A) \tag{13}$$

$$\lambda=-(\gamma-1)^2\rho e(\phi-A)=-(\gamma-1)\mu \tag{14}$$

$$\kappa=\gamma\rho e(\phi-A) \tag{15}$$

and the speed of sound c_s is also defined by

$$c_s=\sqrt{\gamma\frac{p}{\rho}}=\sqrt{\gamma(\gamma-1)e} \tag{16}$$

The transfer coefficients, the speed of sound, and the equation of the equilibrium energy show that the model applied is consistent with the conventional model in which only the translation mode of the energy is considered. Moreover, this model considers the additional degrees of freedom of energy by Eq. (5) without changing the evolution equation of f_i^{eq} ; therefore it is very simple task to add the degree of freedom. The transfer coefficients, the speed of sound, and the equilibrium rotation energy are given by the same expressions in any models other than D2Q21 or models of other lattice shapes or those of other local equilibrium distribution functions f_i^{eq}.

Until now, $G_i^{eq}=Ef_i^{eq}$ in Eq. (4) has been treated as a distribution function of the rotation energy, however it can be defined as a distribution function of any other kinetic energy. For instance, the degree of freedom is limited to the number of the dimension and it can be considered as the additional modes of translation energy for one- and two-dimensional space. In other words, it can be understood as the distribution functions of any energy modes including translation that cannot be expressed by the conventional FDLB models.

3. Some results and Discussion

3.1 Sound speed

The speed of sound simulated by the model applied above is also compared to the theoretical value in Eq. (16) and the conventional FDLB model with 21 velocities. In Fig. 1, it is seen that the speed of sound calculated for the specific heats $\gamma=1.4$, $\gamma=1.67$ and $\gamma=2.0$ agree well with the theoretical values and the conventional FDLB model for various internal energies.

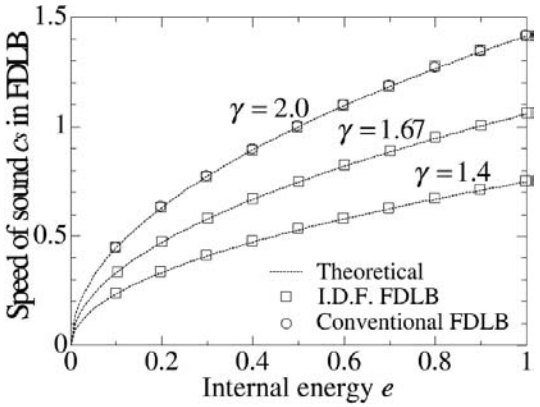

Fig. 1 Speed of Sound for various specific heats

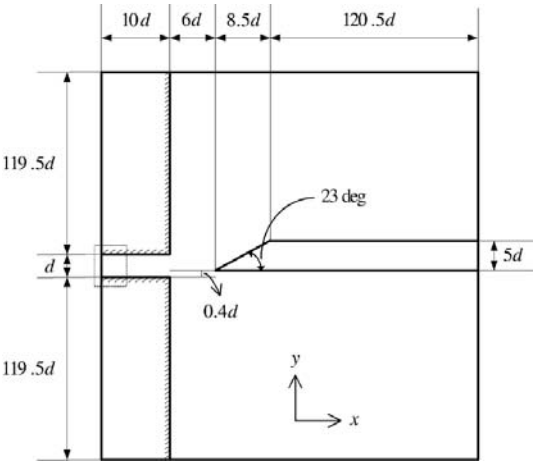

Fig. 2 Edgetone geometry

3.2 Edgetone

In the edge tone, a discrete frequency sound is produced by several flow geometries in which a free shear layer interacts with a solid boundary. One well-known device which produces discrete frequency sound in this way is the edge tone. Its sound is generated because the impinging jet forms a self-excited flow, maintained by a feedback loop. Particularly obvious are the main features by the simplifying considerations first stated by Powell (1961). This edgetone is an effective device for transforming the energy of the jet into acoustic radiation at a discrete frequency, and it is used as the source, which is coupled to a resonator in several wind instruments. Since the last century, the edgetone has been the subject of a large number of both experimental and theoretical investigations. Some books and reviews on edgetones are found in this field (Holger et al., 1977 ; Ohring, 1988 ; Crighton, 1992, Bamberger et al., 2004).

3.2.1 Numerical conditions

The dimension of the edgetone is shown in Fig. 2 and all the length scales are normalized by the width of nozzle d in the computation. Flows are assumed to be laminar with the same incoming velocity. For the hydrodynamic and flow-induced noise calculations, a computational domain is set for $0 \leq x \leq 145d$ and $0 \leq y \leq 240d$ (301×301 mesh cells), and the edge is an angle of $\alpha = 23^0$. For spatial derivatives, a third-order-accurate up-wind scheme (second order accurate at the boundary) is employed and a second-order-accurate Runge-Kutta scehme is used for time integration. Adiabatic and no-slip conditions are employed on the wedge and walls, and an outflow condition is imposed on the outer far field boundary. Computations start with a uniform velocity $u_i(T(=Ut/d)=0)=(U_0,\ 0)$ at the nozzle inlet.

3.2.2 Edgetones involving feedback

The results of FDLBM, adaptive finite element method and experiment (Bamberger et al., 2004) for various inlet velocities (u=3.38 m/s~15 m/s

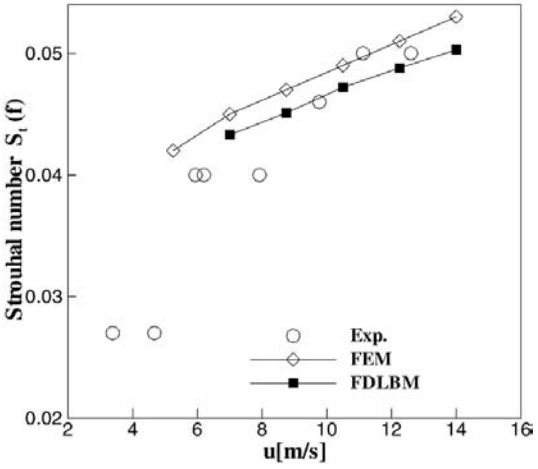

Fig. 3 Comparison of S_t of the frequency for FDLBM, FEM and Experiment (Bamber et al., 2004)

or $M=0.026\sim0.041$, $\gamma=1.4$) at the nozzle with the Strouhal number $S_t(=fd/u)$ are shown in Fig. 3. A comparison for inlet velocities indicates that the FDLBM with an internal degree of freedom is qualitatively compatible with those of FEM and experiment.

In the near-field flow structure, streamlines at three different instants are presented in Fig. 4 for the case of $u=14$ m/s ($M=0.041$) and $\gamma=1.4$. Here, a jet which comes out of the nozzle first collides with the edge since a uniform flow as the initial condition without a turbulence is given, and the jet equally divided itself into the upper and lower sides of the wedge as shown in Fig. 4 (a). Then, the jet begins to fluctuate, colliding with the edge. It fluctuates upward and downward periodically. This fluctuation synchronizes with the period of the vortex, which arises from the top and bottom wall in the vicinity of the nozzle exit. It is considered that, because of the vortex, the fluctuation of the jet is induced. Then with the effect of the jet, the vortex moves toward downstream, and it undulates like the form of the jet by the rotation energy. As a result, the jet changes its direction due to the rotation of the vortex in the vicinity where the vortex exceeded the tip of the wedge, and flows into unilateral sides of the wedge, as shown in Figs. 4(b) and 4(c).

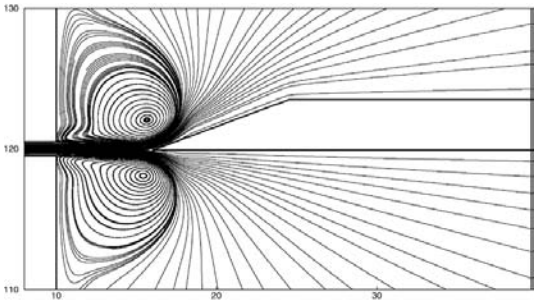

(a) $T(=Ut/d)=20.3$

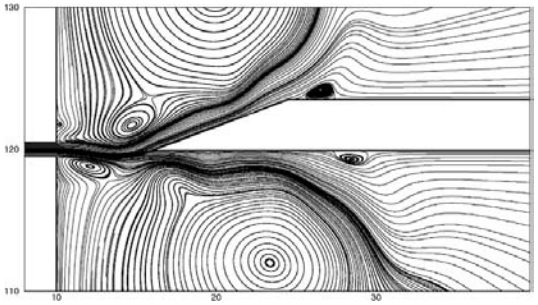

(b) $T(=Ut/d)=151$

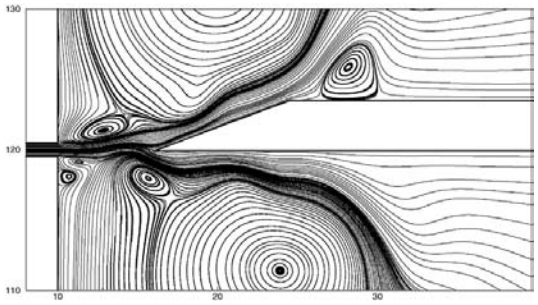

(c) $T(=Ut/d)=164$

Fig. 4 Streamlines for three difference instants at $u=14$ m/s ($M=0.041$) and $\gamma=1.4$

Owing to the fluctuation of this jet as shown in Fig. 4, the pressure on the side exposed to the jet increases (Fig. 5(b)) but, on the opposite side, the pressure decreases (Fig. 5(a)) periodically. In other words, the edgetone is generated because the impinging jet forms a self-excited flow maintained by a feedback loop. As a result, on the upper and lower parts of the edge, the pressure wave with an opposite phase is generated. It is shown that the maximum pressure p_{max} and minimum pressure p_{min} have been observed to be $p_{max}=0.0005$ and $p_{min}=-0.0004$, respectively, at the vicinity of the edge as has been examined by Kayayoglu and Rockwell (1986). This feature is to be explained by the antisymmetry of the downstream disturbance about the central surface of jet. Vortices in the jet impinge on the surface of the wedge to produce a surface-pressure fluctuation, which propagates upstream at the speed of sound to the nozzle. At the outlet of the nozzle, this pressure fluctuation produces vorticity fluctuations in the shear layers of the jet, modifying the rolling up of the shear layers due to the instability. During the two periods, edge vortices are observed above and below the edge, being 180^0 out of phase to each other. In the figures, the vortex is below the edge during the downward movement of the jet. In other words, the vortices in the shear layer impinge on the downstream edge and induce large pressure oscillations, which become the major noise sources. At certain con-

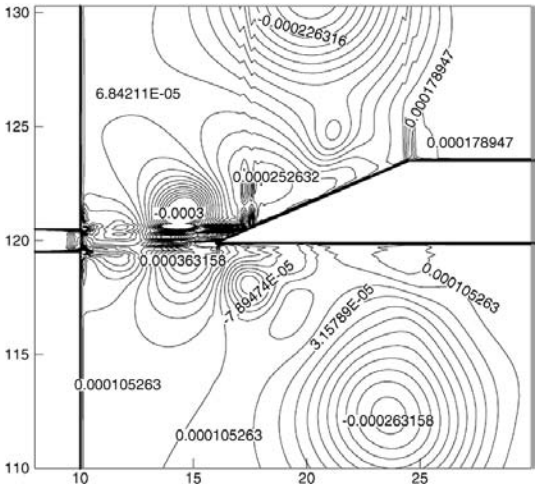

(a) $T(=Ut/d)=151$

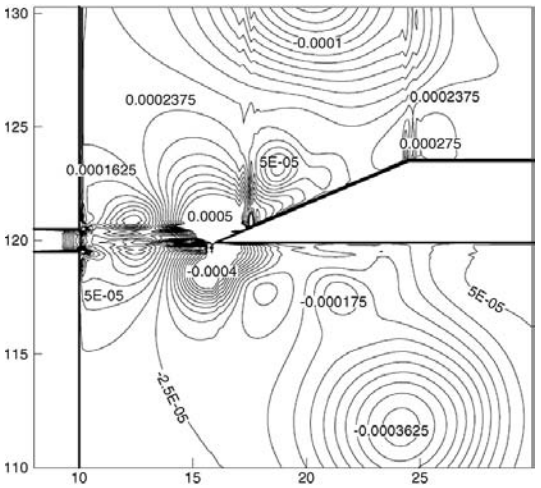

(b) $T(=Ut/d)=164$

Fig. 5 Pressure distribution at two different instants

ditions periodic movement due to positive feedback mechanism occurs, and it creates audible acoustic pressure. In addition, since the sound radiation by the edge is proportional to the surface pressure, the maximum pressure point can be regarded as the effective source point, though the exact point can be somewhat different depending on the radiating direction.

Figure 6 shows a phase diagram $u_1(x_2, 0.6d)$ versus $u_1(x_1, 0.6d)$ with x_2 a point $w/5$ left of x_1. Here, we analyzed the temporal behavior of a typical quantity of flow at a fixed position x_1 after computing for a sufficiently large number of periods. Here, we used x_1, a point $w/5$ left and

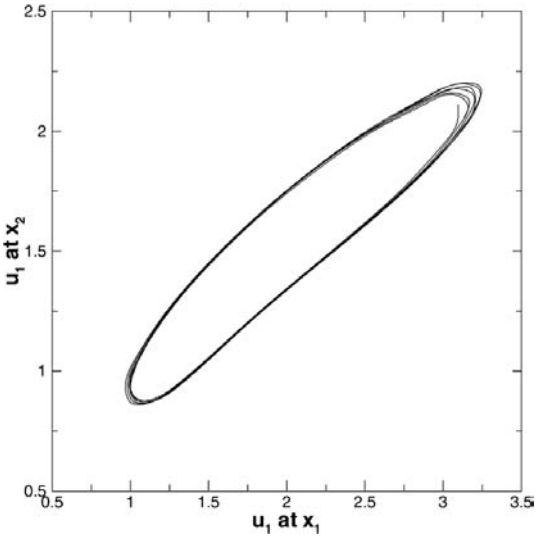

Fig. 6 Phase diagram $u_1(x_2, 0.6d)$ versus $u_1(x_1, 0.6d)$ with x_2 a point $w/5$ left of x_1 at $u=12.25$ m/s

slightly above the edge of the labium. For quantity we chose the horizontal velocity component $u_1(x_1, 0.6d)$ at x_1, and it certainly demonstrates the periodic behavior of the flow.

The time variations of the acoustic pressure at 2 points in calculating area are shown in Fig. 7 for the case of $M=0.036(\cong 12.25$ m/s) and 0.041 ($\cong 14$ m/s), respectively. The observation points are radically considered on the edge tip (x_0, y_0), in which these points apart from $(109d, \pm 100d)$ in the x and y direction, respectively. The solid line is the upper side of the wedge, and the dotted one is the lower side of the wedge, and the sound signals fluctuate with a period of $\Delta T(=Ut/d)=20.48$ and 19.88, which corresponds to $S_t(=fd/U)=0.049$ and 0.051, respectively. Moreover, it can be confirmed that the amplitude of the fluctuations of the acoustic pressure in the points is about 0.00006, and it has a more minute value than the pressure fluctuation at the vicinity of the edge with 0.0009.

In case of $M=0.2(\cong 64$m/s), Fig. 8 shows the acoustic pressure field for three different instants ($T=Ut/d=260$ and 268), where the contour level Δp_{step} fluctuates from -0.001 to 0.002. We can see in the figure, the positive and negative acoustic pressure propagates symmetrically in the

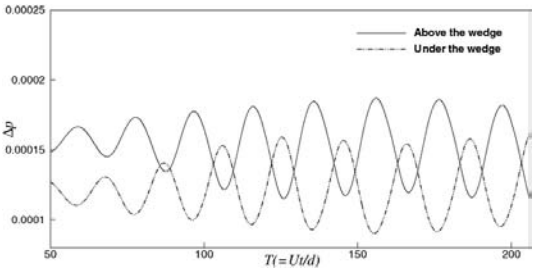

(a) $M=0.039$ ($\cong$12.25 m/s)

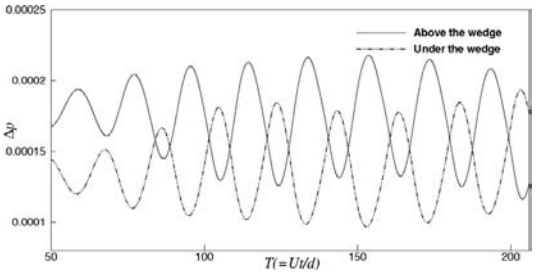

(b) M=0.041 ($\cong$14.0 m/s)

Fig. 7 Time variation of acoustic pressure for two different Mach number. $\gamma=1.4$

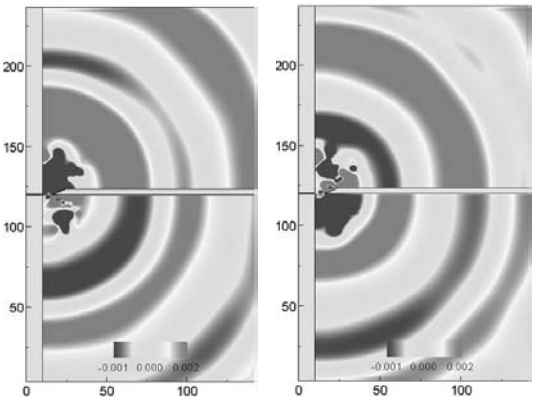

(a) $T(=Ut/d)=260$ (b) $T(=Ut/d)=268$

Fig. 8 Acoustic pressure field at $M=0.2$ ($\cong$68 m/s) and $\gamma=1.4$

upper and lower parts of the wedge alternately.

4. Conclusions

Direct simulation of flow-induced noise is approached by applying the finite difference-based lattice Boltzmann method with an internal degree of freedom, which was introduced by Ref. (1999) in LBM. The present method correctly predicts the frequency characteristics of the discrete oscillation of a jet-edge feedback cycle for various inflow velocities ($u=3.38$ m/s$\sim$15 m/s or $M=0.026\sim0.041$, $\gamma=1.4$ and $u=68$ m/s or $M=0.2$). We have succeeded in capturing very small pressure fluctuations resulting from periodically oscillation of jets around the edge with an angle of $\alpha=23^0$. Its interaction with the edge produces an irrotational feedback field which, near the nozzle exit, is a periodic transverse flow.

Acknowledgments

This work was supported by the Korea Research Foundation Grant (KRF-2004-003-D00060), in which main Calculations were performed by using the supercomputing resources of the Korea Institute of Science and Technology Information (KISTI).

References

Alexander, F. J., Chen, S. and Sterling, D. J., 1993, "Lattice Boltzmann Thermodynamics," *Physical Review E*, Vol. 47, pp. 2249$\sim$2252.

Bamber, A., Bansch, E. and Siebert, K.G., 2004, "Experimental and Numerical Investigation of Edge Tones," *ZAMM. Angew. Math. Mech.*, Vol. 84, No. 9, pp. 632$\sim$646.

Cao, N., Chen, S., Jin, S. and Martinez, D., 1997, "Physical Symmetry and Lattice Symmetry in the Lattice Boltzmann Method," *Physical Review E*, 55, pp. R21$\sim$R24.

Chen, Y. and Doolen, G. D., 1998, "Lattice Boltzmann Method for Fluid Flows," *Annual Review Fluid Mechanics*, Vol. 30, pp. 329$\sim$364.

Crighton, D. G., 1992, "The Jet Edge-Tone Feedback Cycle; Linear Theory for the Operating Stages," *Journal of Fluid Mechanics*, Vol. 234, pp. 361$\sim$391.

Holger, D. K., Wilson, T. A. and Beavers, G. S., 1977, "Fluid Mechanics of the Edgetone," *Journal of Acoustical Society of America*, Vol. 62(5), pp. 1116$\sim$1128.

Kang, H. K., Tsutahara, M., Ro, K. D. and Lee, Y. H., 2002, "Numerical Simulation of Shock Wave Propagation Using the Finite Difference

Lattice Boltzmann Method," *KSME International Journal*, Vol. 16, No. 10, pp. 1327～1335.

Kaykayoglu, R. and Rockwell, D., 1986, "Unstable Jet-Edge Interaction. Part 1. Instantaneous Pressure Fields at a Single Frequency," *Journal of Fluid Mechanics*, Vol. 169, pp. 125～149.

Ohring, S., 1988, "Calculations Pertaining to the Dipole Nature of the Edge Tone," *Journal of Acoustical Society of America*, Vol. 83, pp. 2047～2085.

Peng, G., Xi, H., Duncan, C. and Chou, S. H., 1999, "Finite Volume Scheme for the Lattice Boltzmann Method on Unstructured Meshes," *Physical Review E*, Vol. 59, pp. 4675～4681.

Powell, A., 1961, "On the Edge Tone," *Journal of Acoustical Society of America*, Vol. 33, pp. 395～409.

Takada, N. and Tsutahara, M., 1999, "Proposal of Lattice BGK Model with Internal Degrees of Freedom in Lattice Boltzmann Method," *Trans. JSME Journal*, B, Vol. 65, No. 629, pp. 92～99.

Tsutahara, M., Takada, N. and Kataoka, T., 1999, Lattice Gas and Lattice Boltzmann Methods. *Corona-sha* ; in Japanese.

Wolfram, S., 1986, "Cellular Automaton Fluids 1 ; Basic Theory, " *Journal of Statistical Physics*, Vol. 45, pp. 471～526.